Sys Rev Pharm 2020;11(12):1456-1463
A multifaceted review journal in the field of pharmacy

THE GEOMETRY AND OPTICAL MODELS OF THE ERYTHROCYTE

K.A. Shapovalov[1]

1Department of Medical and Biological Physics, Krasnoyarsk State Medical University named after Prof. V.F. Voyno-Yasenetsky, Partizana Zheleznyaka Street, 1, Krasnoyarsk, 660022, Russia
Received:, Revised:, Accepted:

ABSTRACT
The main axisymmetric geometrical models of erythrocyte's surface are considered. Usually the axisymmetric models have cross-sections as ellipses, Cassinian Ovals, polynomial curves. Such geometrical models are often based of optical models and applied for the description of 3D erythrocyte's shape in scanning flow cytometry. We are suggested to use more strict and complicated Perseus curves for the description of cross-sections of the erythrocyte. The formulas for the volume, surface and cross-section areas in the proposed erythrocyte's model of Perseus curves are obtained. We are revealed that the Perseus curves are approximated to experimental polynomial curves more exact than the Cassinian Ovals. We are numerically compared the phase function of light scattering by the individual erythrocyte in the Rayleigh-Gans-Debye approximation for all main optical models of the red blood cell. The good agreement is demonstrated for the phase function of light scattering by the erythrocyte for the Perseus curves' model in comparison with polynomial models in the Rayleigh-Gans-Debye approximation.

Keywords: light scattering, red blood cell (corpuscle), scanning flow cytometry.

INTRODUCTION

IMPORTANCE OF THE PROBLEM

The scattering of electromagnetic waves by dielectric particles is an important problem for a variety of applications ranging from particle sizing and remote sensing, astrophysics to radar meteorology and biological sciences. So, in the area of medical diagnostics, understanding how a laser or light beam interacts with blood suspensions or a whole-blood medium is of paramount importance in quantifying the inspection process of precision in many commercial devices and experimental setups that are used widely for in vivo or in vitro blood measurements [1 - 4].

FRAMEWORK OF THE PROBLEM

Many colloidal, biological and aerosol particles of great interest in nature are such that their refractive index m, relative to the surrounding medium is sufficiently close to unity [1, 2]. The particles satisfying the condition $|m-1|<<1$ (where $m=n+i\chi$ is its relative refractive index) are generally termed as optically "soft" particles. Otherwise, the assumption of "soft" particles suggests that the refraction and reflection of the rays passing through the particle are negligible and that the absorption is not very strong. Note that for red incident light $\lambda = 650\ nm$ (where λ is the wavelength of light) the real part of relative refractive index of an erythrocyte n is varied from 1.04 to 1.05 and the imaginary part χ is varied from 0.001 to 0.007 (see [3, 5]). Therefore, the alone erythrocyte is often assumed as an optically "soft" particle. If light scattering particles are optically "soft" then the Rayleigh–Gans–Debye (RGD) [1, 3, 6], Anomalous Diffraction (AD), or Wentzel–Kramers–Brillouin (WKB) approximations can be applied [3, 5, 7]. The RGD approximation (known as the first Born approximation in quantum mechanics) is valid when the phase shift Δ is much smaller compared with unity $\Delta<<1$, where we use so-called "phase shift" of central ray Δ ($\Delta = 2ka|m-1|$, where a is the longest dimension through the particle, $\mathrm{k}=2\pi/\lambda$ is the wavenumber). The application of the AD approximation is restricted with the phase shift Δ greater than unity $\Delta>1$. The range of validity of the WKB approximation is included ranges of validity of both the RGD and AD approximations [5, 7]. But in all declared approximations we need to know the correct size, surface, volume of particle (or erythrocytes).

THE PURPOSE OF RESEARCH

The purpose of this research is to consider main geometrical models of erythrocyte's surface and choose

more adequate and suitable for effective calculation of light scattering characteristics.

GEOMETRICAL MODELS OF ERYTHROCYTE'S SURFACE

The main object of the immense majority of medical diagnostics is a erythrocyte (or red blood cell (RBC), red blood corpuscle). The shape of RBC is researched and described earlier in the numerous papers [8 - 13]. The profile (or the axial cross-section) of RBC is shown in Figure 1. Usually, RBCs measure from 6.6 to 8.0 μm in diameter, however, cells with a diameter greater than 9 μm (macrocytes) or less than 6 μm (microcytes) have been observed. Some average parameters of normal RBC are wrote in Table 1.

Table 1. Average geometric parameters of normal Red Blood Cells

Source	Diameter D, μm	Minimal Thickness, μm	Maximal Thickness, μm	Surface Area, μm^2	Volume, μm^3	Sphericity Index
Ponder[11]	8.50	1.00	2.40	152.00	112.00	0.740
Skalak[9]	8.40	0.85	2.04	141.61	91.52	0.694
Tchijevsky[8]	7.50	0.85	1.875	108.68	62.96	0.704
Fung[11]	7.65	1.44	2.84	129.95	97.91	0.792
Evans[10]	7.82	0.81	2.58	135.00	94.00	0.742
Gilev[14]	6.42	1.90	3.03	101.10	77.80	0.80

The difference in diameters of normal RBCs is explained by their range in age and other reasons.

The well-known average polynomial curve have been obtained by Skalak in [9]:

$$ZSka(x,R) = \pm 0.86R\sqrt{(1-x_R^2)}(0.0130693\,x_R^4 + 0.284292\,x_R^2 + \text{,} \quad (1)$$

where $x_R = x/R$ and R is a average radius of RBC.

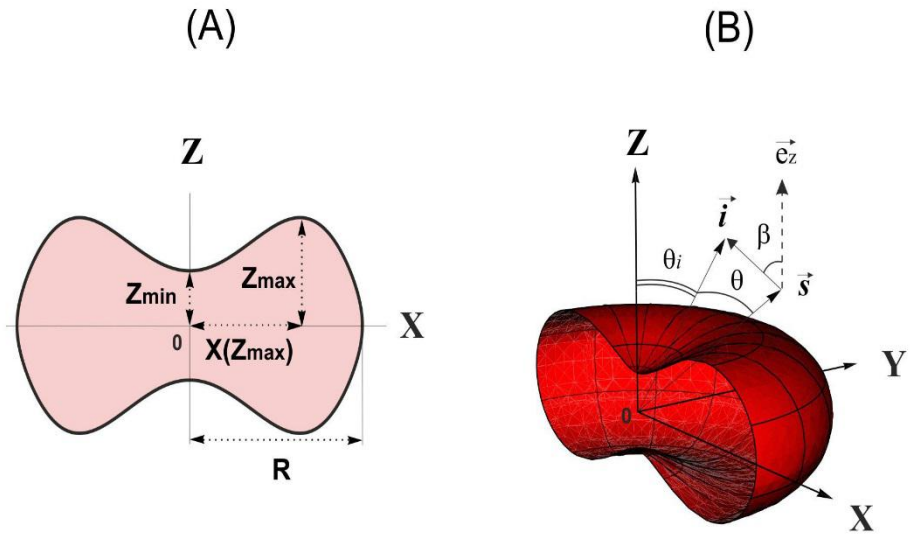

Figure 1. The profile (or the axial cross-section) of erythrocyte (A) with main parameters such as the radius R, the half of maximal $Zmax$, minimal thickness $Zmin$, the X position of $Zmax$ (or $X(Z_{max})$) and the coordinate system for the task of light scattering (B) (where the unit vectors $\vec{s}$ and $\vec{i}$ are aligned with the light scattering and propagation directions, respectively). But in earlier work of Tchijevsky [8] we are found such polynomial curve

$$ZChi(x,R) = \pm R\sqrt{\frac{1}{64} + \frac{27}{128}x_R^2 - \frac{243}{1024}x_R^4 + \frac{891}{25600}x_R^2\left(x_R^2 - \frac{4}{9}\right)^2}. \quad (2)$$

The third average polynomial curve proposed by Fung [11] and modified in [15, 16] can be written as

$$ZFun(x,R) = \pm \varepsilon R\sqrt{1-x_R^2}\left(0.1583 + 1.5262x_R^2 - 0.8579x_R^4\right), \quad (3)$$

where ε is an aspect ratio of maximum thickness and diameter, in [15] is equal to 0.65, in [16] is equal to 0.52. For $\varepsilon = 0.65$ we have

$$ZFun(x,R) = \pm R\sqrt{1-x_R^2}\left(0.102895 + 0.99203x_R^2 - 0.557635x_R^4\right)$$ The last modification of the polynomial Fung's curve [11] we found in [17]:

$$ZGil(x,R) = \pm R\sqrt{1-x_R^2}\left(0.187 + 1.035x_R^2 - 0.774x_R^4\right). \quad (4)$$

The transformation of equations (1) and (2) yield us next expressions for the comparison of polynomial curves

$$ZSka(x,R) \approx \pm R\sqrt{1-x_R^2}\left(0.101176 + 0.988498x_R^2 - 5.82015x_R^4\right), \quad (5)$$

$$ZChi(x,R) \approx \pm R\sqrt{1-x_R^2}\left(0.125 + 0.93375x_R^2 - 3.62678x_R^4\right). \quad (6)$$

The marked difference in the values is noted for expansion's terms of forth degree between equations (5) and (6).

Of course, the Cassinian Ovals (also termed the Cassinian Oval) are useful and convenient models of erythrocyte's shape [12, 13, 18], because they have two parameters *a* and *c* for changing the shape of erythrocyte under different pathological conditions $(a < c < a\sqrt{2})$.

In Cartesian coordinates we can write [13]

$$ZCas(x,a,c) = \pm a\sqrt{\sqrt{\left(\frac{c}{a}\right)^4 + 4\left(\frac{x}{a}\right)^2} - \left(\frac{x}{a}\right)^2 - 1}, \quad (7)$$

or in polar coordinates

$$\rho Cas(\theta,a,c) = a\sqrt{\cos(2\theta) + \sqrt{\left(\frac{c}{a}\right)^4 + \cos^2(2\theta) - 1}},$$

where $0 < \theta < 2\pi$.

The Perseus Curves (or the spiric sections of Perseus) are more perfect models of erythrocyte's shape than the Cassinian Ovals but they have already three parameters *p, q, r* [21, 22]. The Perseus Curves include the Cassinian Ovals as a private case. Such more complicated model is necessary, for instance, see the adding factor (third "unusual" parameter) in [12] for correction of the Cassinian Ovals and best approximation with experimental results or parametric equations in [23, 24, 25].

The Perseus Curves in Cartesian coordinates are defined by

$$ZPer(x,p,q,r) = \pm q\sqrt{\frac{r^2-p^2}{q^2} + \sqrt{\left(\frac{2p}{q}\right)^2 + 4\left(\frac{x}{q}\right)^2} - \left(\frac{x}{q}\right)^2 - 1}, \quad (8)$$

in polar coordinates

$$\rho Per(\theta,p,q,r) = q\sqrt{\cos 2\theta + \frac{r^2-p^2}{q^2} + \sqrt{2\left(\frac{r^2+p^2}{q^2} + \frac{r^2-p^2}{q^2}\cos 2\theta\right) + \cos^2(2\theta) - 1}}$$

Note when the condition $p = r$ is true then the Perseus Curves change into the Cassinian Ovals. Using formulas $P' = 2\left(p^2 - r^2 - q^2\right)$, $Q' = 2\left(q^2 + p^2 - r^2\right)$, $R' = \left((p+q)^2 - r^2\right) \times \left((p-q)^2 - r^2\right)$, we can transform from the equation (8) of Perseus Curves to the parametric equations' notation in [23].

Besides, we can apply the simple model proposed by Borovoi A.G. in [20] on the basis of Roses or Grandi's Curves. In polar coordinates we have an upper or bottom (sign is plus or minus respectively) half of vertically located erythrocyte [20]

$$\rho Bor(\theta,a,b) = \pm\left(a\sin^5\theta + b\right), \quad (9)$$

where $0 < \theta < \pi$ and $R=a+b$ is a maximal radius of RBC,

after RBC's rotation from vertical to the horizontal position we obtain from (9)

$$\rho Bor(\theta,a,b) = \begin{cases} a\cos^5\theta + b, & \text{provided } -\pi/2 < \theta < \pi/2, \\ -a\cos^5\theta + b, & \text{provided } \pi/2 < \theta < 3\pi/2, \end{cases} \quad (10)$$

and in spherical coordinates (r,θ,φ) [20] write as

$$rBor(\theta,\varphi,a,b)=a\sin^5\theta+b. \quad (11)$$

Also the parametric function for the Borovoi's model can be written as

$$\left(x^2+z^2\right)^3=\pm ax^5+b\left(x^2+z^2\right)^{\frac{5}{2}},$$

where $x>0$.

We summarize known geometric parameters of RBC (see also Figure 1) for the Cassinian Ovals [13, 18] and new formulas obtained by author for the Perseus Curves (provided that $p\neq q$ and $q-r<p<q+r$) in the next collated Table 2. Obviously, the volume, surface and the cross-section areas of the Perseus Curves when $p=r$ change into corresponding formulas of the Cassinian Ovals (see Table 2).

For the simple transition from formulas of the Perseus Curves to the Cassinian Ovals' notations use expressions $p=r=\frac{c^2}{2a}$,

$$s_0=q=a,\quad k_0=\sqrt{\frac{c^2+a^2}{2c^2}},\quad k_2=\frac{a^2}{c^2},\quad \alpha_0=\frac{c^2+a^2}{2c^2}=k_0^2,\quad \phi_0=\arcsin\sqrt{\frac{2a^2}{c^2+a^2}}$$

Table 2. The geometric parameters of erythrocyte for the Perseus Curves and Cassinian Ovals

Parameter	Perseus Curves	Cassinian Ovals [13, 18]
Half of maximal thickness, *Zmax*	r	$\frac{c^2}{2a}$
Half of minimal thickness, *Zmin*	$\sqrt{r^2-(q-p)^2}$	$\sqrt{c^2-a^2}$
Radius, $R = Xmax$	$\sqrt{(q+r)^2-p^2}$	$\sqrt{c^2+a^2}$
X position of *Zmax*	$\sqrt{q^2-p^2}$	$\frac{1}{2a}\sqrt{4a^4-c^4}$
Volume, *V*	$2\pi q\left\{Z_{min}\left(2(q-p)-\lvert q-p\rvert+\frac{2}{3q}Z_{min}^2\right)+r^2\arccos\left(\frac{p-q}{r}\right)\right\}$	$\pi\left\{\frac{\sqrt{c^2-a^2}(2a^2+c^2)}{3}+\frac{c^4}{2a}\arccos\left(1-2\left(\frac{a}{c}\right)^2\right)\right\}$
Suface Area, S_{SA}	$4\pi r\{s_0+s_1+(q-p-r)(s_2+s_3)\}$, where $s_0=\frac{2qr}{\sqrt{p^2-r^2}}\tanh^{-1}\left(\sqrt{\frac{p-r}{p+r}}\right)$, $s_1=2\sqrt{pq}E(\phi_0,k_0)$, $s_2=p/r-1$, $s_3=\frac{q}{\sqrt{pq}}\left(F(\phi_0,k_0)-\frac{r}{p+r}\Pi(\alpha_0,\phi_0,k_0)\right)$, $\phi_0=\arcsin\sqrt{\frac{2q}{q+p+r}}$, $\alpha_0=\frac{q+p+r}{2(p+r)}$, $k_0=\sqrt{\frac{(q+p)^2-r^2}{4pq}}$	$4\pi\frac{\sqrt{2}c^3}{a}\left\{E(\phi_0,k_0)-\frac{c^2-a^2}{2c^2}F(\phi_0,k_0)\right\}$, where $\phi_0=\arcsin\sqrt{\frac{2a^2}{c^2+a^2}}$, $k_0=\sqrt{\frac{c^2+a^2}{2c^2}}$

Cross-Section Area, S_{CS}	$2\left(p^2-r^2\right)\left(2E(\phi_1,k_1)s_4+\frac{2F(\phi_1,k_1)}{k_2}s_5-\pi\right)$ $+4q\sqrt{rp}\left(E(k_2)-K(k_2)\right)$ $+2(p+r)(q+p-r)\sqrt{\frac{r}{p}}K(k_2)$, where $s_4=k_2\left(K(k_2)+iK(k_2')\right)-iK(k_1)$, $\phi_1=\arcsin\sqrt{\frac{q+p-r}{q+p+r}}$, $k_1=\sqrt{\frac{q^2-(p+r)^2}{q^2-(p-r)^2}}$, $k_2=\sqrt{\frac{q^2-(p-r)^2}{4pr}}$, $k_2'=\sqrt{\frac{(p+r)^2-q^2}{4pr}}$.	$2c^2E\left(k_2\right)$, where $k_2=\frac{a^2}{c^2}$

Notations $F(\phi,k),E(\phi,k),\Pi(\alpha,\phi,k)$ are incomplete elliptic integrals of the first, second, third kinds respectively and $K(k)=F(\pi/2,k),E(k)=E(\pi/2,k)$ are complete elliptic integrals of the first, second kinds respectively [19].

NUMERICAL RESULTS AND DISCUSSION

COMPARISON OF THE MODELS OF ERYTHROCYTE GEOMETRICAL PROFILE

Let us compare all these models under given conditions, for known three parameters: the diameter $D=2R$, the minimal $2Z_{min}$ and maximal thickness $2Z_{max}$ of RBC.

$$c=\sqrt{\frac{R^2+Z_{min}^2}{2}},\qquad a=\sqrt{\frac{R^2-Z_{min}^2}{2}}. \tag{12}$$

From equation (8) for the parameters of the Perseus Curves we find

$$q=\frac{\left(R^2-Z_{min}^2\right)\left(Z_{max}-\sqrt{Z_{max}^2-Z_{min}^2}\right)}{2Z_{min}^2},\qquad p=q-\sqrt{Z_{max}^2-Z_{min}^2}. \tag{13}$$

For polynomial geometrical profiles of RBC with $Z(x)$ [11] the volume was calculated as

$$V(R)=4\pi\int_0^R xZ(x)dx, \tag{14}$$

the surface area was computed as

$$SA(R)=4\pi\int_0^R x\sqrt{1+\left(\frac{dZ(x)}{dx}\right)^2}\,dx, \tag{15}$$

the sphericity index was computed as

$$SI(R)=\frac{\sqrt[3]{36\pi V(R)^2}}{SA(R)}. \tag{16}$$

The numerical results of geometrical profiles are shown in Figure 2 for all described models with common parameters $Z_{min}=0.385\mu m$, $Z_{max}=0.91\mu m$, $X_{max}=R=3.75\mu m$.

Of course, all models (except the Cassinian Ovals, the Perseus Curves and the Borovoi's model) will be multiplied by individual aspect ratio coefficient ε for the strict equality of given Z_{min}.

Using equation (7), for the parameters of the Cassinian Ovals we obtain

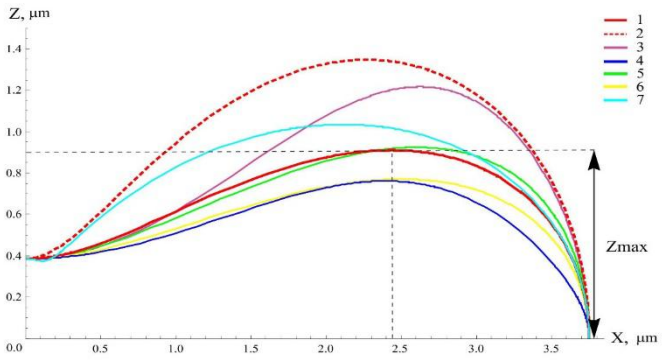

Figure 2. The comparison of geometrical profiles for the models of erythrocyte calculated by means of equations: **1** - Eq.(8) Perseus Curves, **2** - Eq.(7) Cassinian Ovals, **3** - Eq.(3) Yurkin[15], **4** - Eq.(4) Gilev[17], **5** - Eq.(1) Skalak [9], **6** - Eq.(2) Tchijevsky [8], **7** - Eq.(10) Borovoi [20] with parameters

$Z_{min} = 0.385\mu m$, $Z_{max} = 0.91\mu m$, $X_{max} = R = 3.75\mu m$.

The sphericity index, the volume and the surface area of RBC calculated for given parameters Z_{min}, Z_{max}, R in the model of the Cassinian Ovals and others are written in Table 3.

Moreover, note that the calculations in the Cassinian Ovals' model with equation (7) yield significantly larger value of $Z_{max} \approx 1.35\mu m$ than one in other profiles for RBC with given Z_{min} and *R* (see Figure 2).

$Z_{min} = 0.385\mu m$, $Z_{max} = 0.91\mu m$, $X_{max} = R = 3.75\mu m$.

Table 3. The surface area, the volume, the sphericity index calculated in the models of erythrocyte with parameters

Model	Surface Area, μm^2	Volume, μm^3	Sphericity Index	Aspect Ratio ε
Perseus Curves	110.16	64.69	0.707	-
Cassinian Ovals	124.48	94.21	0.804	-
Yurkin [15]	122.73	82.05	0.744	0.649
Gilev[14]	102.38	51.43	0.653	0.549
Skalak [9]	112.49	66.13	0.703	0.873
Tchijevsky [8]	105.96	55.39	0.663	0.821
Borovoi [20]	111.76	72.79	0.754	-

LIGHT SCATTERING AMPLITUDE AND PHASE FUNCTION

Let the symmetry axis of a static homogeneous erythrocyte of height $2Z_{max}$ and radius R be aligned with the Z axis and a plane electromagnetic wave be incident in the ZOX plane of the Cartesian coordinate system at the angle θ_i to the Z axis (see Figure 1 (B)):

$$\vec{E}_i(r) = \vec{e}_i \exp[ik(x\sin\theta_i + z\cos\theta_i)], \quad (17)$$

where $k = 2\pi/\lambda$ is the wavenumber and the unit vector $\vec{e}_i$ is aligned to the incident-wave polarization.

Forth we use the light-scattering amplitude for the RGD approximation [3 - 6] in scalar form

$$f(\theta,\beta) = \frac{k^2|P|}{4\pi}\int_V (m^2-1)T(m,\theta_i)\exp[i\vec{k}_s\cdot\vec{r}]dV, \quad (18)$$

where the unit vectors $\vec{s}$ and $\vec{i}$ are aligned with the light scattering and propagation directions, respectively, $\vec{k}_s = k(\vec{i}-\vec{s})$, $|\vec{k}_s| = 2k\sin\frac{\theta}{2}$, $T = T(m,\theta_i)$ is the Fresnel transmission coefficient, where $T(m,\pi/2) = 2/(m+1)$, θ is the angle between vectors $\vec{i}$ and $\vec{s}$, β is the angle between axis Z and vector $\vec{k}_s$, $|P| = |[-\vec{s}\times(\vec{s}\times\vec{e}_i)]$ (for brief expression suppose that in a scalar form $|P| = 1$) and $\vec{r}$ is the radius-vector of a point inside the particle.

So, the phase function [or element of scattering matrix f_{11}] for natural incident light (unpolarized or arbitrary polarized light) provided that $\beta = 0$ is calculated by a formula [1, 7]

$$f_{11}(\theta,0) = k^2 \left| f(\theta,0) \right|^2 \frac{1+\cos^2\theta}{2}, \quad (19)$$

where $\left| f(\theta,\beta) \right|^2$ is a square of modulus of light scattering amplitude.

Further the phase function of light scattering is normalized on the value in a forward direction.

The logarithms of normalized phase functions $Log_{10}(f_{11}[\theta,0]/f_{11}[0,0])$ for the incident light perpendicular and along the axis of RBC's symmetry calculated by means of models in the RGD approximation such as the Perseus Curves, the Cassinian Ovals and others are shown in Figure 3. Note

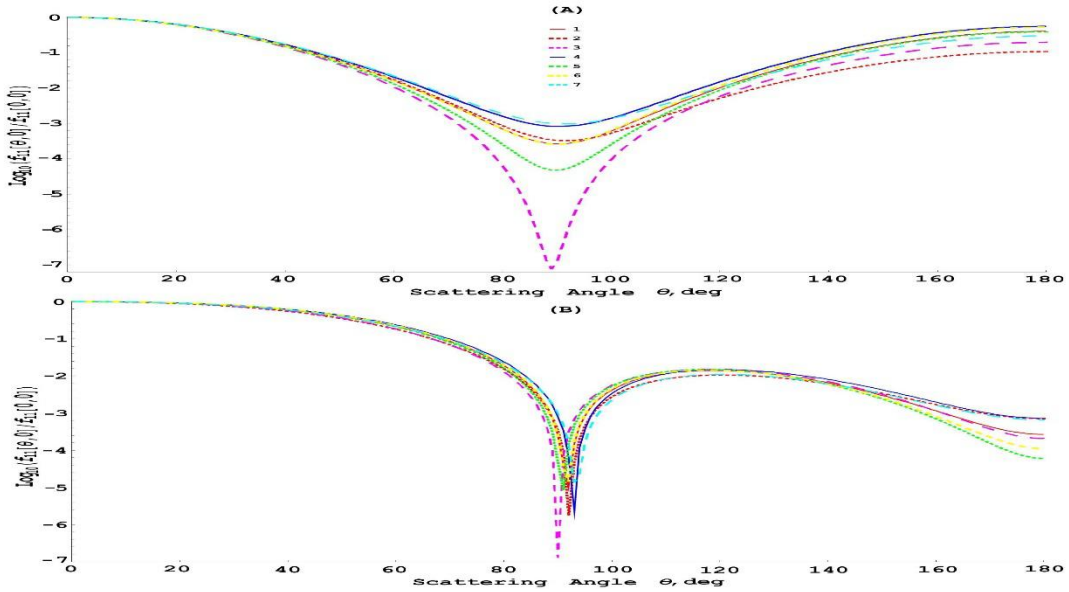

Figure 3. The logarithm of normalized phase function $Log_{10}(f_{11}[\theta,0]/f_{11}[0,0])$ vs. scattering angle θ in the RGD approximation with relative refractive index $m = 1.058 + i0.0001$ and parameters $Z_{min} = 0.385\mu m$, $Z_{max} = 0.91\mu m$, $X_{max} = R = 3.75\mu m$ for incident light along (A) and perpendicular (B) to the axis of erythrocyte's symmetry calculated by means of model equations:

1 - Eq.(8) Perseus Curves, **2** - Eq.(7) Cassinian Ovals, **3** - Eq.(3) Yurkin [15], **4** - Eq.(4) Gilev[17],
5 - Eq.(1) Skalak [9], **6** - Eq.(2) Tchijevsky [8], **7** - Eq.(10) Borovoi [20].

That the normalized phase functions of RBC calculated with equation (3) from Yurkin [15] and the Cassinian Ovals are significant differed from other models in the ranges of scattering angles near 90 and 180 degrees (see Fig. 3). Obviously, such behavior of phase functions of RBC is caused by the Cassinian Ovals and the equation (3) of Yurkin [15] have more abrupt geometric profiles than others (see Figure 2).

CONCLUSIONS

The axisymmetric geometrical models of erythrocyte's surface are considered. We are proposed to use more strict and complicated Perseus curves for the description of cross-sections of the RBC. The expressions for the volume, the surface and cross-section areas in the erythrocyte's model of Perseus curves are obtained. The formulas for the surface and cross-section areas of the Perseus curves' model are included elliptic integrals. After the numerical comparison of geometrical profiles and parameters we are confirmed that the Perseus curves are approximated to experimental polynomial curves more exact than the Cassinian Ovals. We are numerically compared the phase functions of light scattering by the individual erythrocyte in the RGD approximation for scrutinized models of red blood cell. The better agreement is demonstrated for the phase function of light scattering by the erythrocyte in the RGD approximation for the Perseus curves' model than the Cassinian Ovals in comparison with other models.

Over a long-term perspective the numerical comparison of the phase functions of light scattering in the RGD approximation may be generalized for the WKB approximation too.

REFERENCES

1. M. Kerker, The scattering of light and other electromagnetic radiation, Academic Press, New York, London, 1969.
2. S.K. Sharma and D.J. Somerford, Light Scattering by Optically Soft Particles: Theory and Applications, Springer-Praxis, Berlin, Heidelberg, New York, 2006.

A. Ishimaru, Wave Propagation and Scattering in Random Media. v.1. Single scattering and transport theory, Academic Press, New York, 1978.

3. C.F. Bohren, D.R. Huffman, Absorption and Scattering of Light by Small Particles, Wiley, New York, 1998. DOI:10.1002/9783527618156
4. A.N. Shvalov et al., Light-scattering properties of individual erythrocytes, Appl. Opt., 38, no.1, 230-235 (1999). DOI:10.1364/AO.38.000230
5. K.A. Shapovalov, Light scattering by particles with axis of symmetry in Rayleigh-Gans-Debye approximation, J. Sib. Fed. Univ. Math. Phys., 5, no. 4, 586-592 (2012). (in Russian) http://elib.sfu-kras.ru/bitstream/2311/3112/1/shapevalev.pdf
6. K.A. Shapovalov, Extinction and absorption efficiency factors of a finite-length cylinder in the Discrete Dipole and Wentzel-Kramers-Brillouin Approximations, Int. J. Civ. Eng. Technol., 9(8), 1664-1673 (2018). http://www.iaeme.com/ijciet/IJCIET_Paper.asp?sno=12856
7. A.L. Tchijevsky, Structurnyi analiz dvizhuscheysya krovi, Akademia Nauk USSR, Moscow, 1959. (in Russian). https://search.rsl.ru/ru/record/01005406229
8. R. Skalak, A. Tozeren, R.P. Zarda, S. Chien, Strain energy function of red blood cell membranes, Biophys. J., 13, no.3, 245-264 (1973). DOI:10.1016/S0006-3495(73)85983-1
9. E. Evans, Y.C.Fung, Improved Measurements of the Erythrocyte Geometry, Microvasc. Res., 4, no.4, 335-347 (1972). DOI:10.1016/0026-2862(72)90069-6
10. Y.C. Fung, W.C. Tsang, P. Patitucci, High-resolution data on the geometry of red blood cells, Biorheology, 18, no.3-6, 369-385 (1981). DOI:10.3233/BIR-1981-183-606
11. J. Hellmers, E. Eremina, T. Wriedt, Simulation of light scattering by biconcave Cassini ovals using the nullfield method with discrete sources, J. Opt. A: Pure Appl. Opt., 8, 1-9 (2006). DOI:10.1088/1464-4258/8/1/001
12. B. Angelov and I.M. Mladenov, Geometry, Integrability and Quantization, eds. I.M. Mladenov and G.Naber, Coral Press, Sofia, (2000), 27-47. https://projecteuclid.org/euclid.pgiq/1433524876
13. K.V. Gilev et al., Advanced Consumable-Free Morphological Analysis of Intact Red Blood Cells by a Compact Scanning Flow Cytometer, Cytometry Part A, 91A, 867-873 (2017). DOI:10.1002/cyto.a.23141
14. M.A. Yurkin et al. Experimental and theoretical study of light scattering by individual mature red blood cells by use of scanning flow cytometry and a discrete dipole approximation, Appl. Opt., 44, 5249-5256 (2005). DOI:10.1364/AO.44.005249
15. T. Wriedt, J. Hellmers, E. Eremina, R. Schuh, Light scattering by single erythrocyte: Comparison of different methods, J. Quant. Spectrosc. Radiat. Transf., 100, 444-456 (2006). DOI:10.1016/j.jqsrt.2005.11.057
16. K.V. Gilev, E. Eremina, M.A. Yurkin, V.P. Maltsev, Comparison of the discrete dipole approximation and the discrete source method for simulation of light scattering by red blood cells, Opt. Express, 18, no.6, 5681-5690 (2010). DOI:10.1364/OE.18.005681
17. H. Vayo, Some Red Blood Cell Geometry, Canadian J. Physiol. Pharmacol., 61, 646-649 (1983). DOI:10.1139/y83-099
18. M. Abramowitz and I.A. Stegun (eds.), Handbook of mathematical functions, 10th ed., Dover Publications, New York, 1972.
19. A.G. Borovoi, E.I. Naats, U.G Oppel, Scattering of light by a red blood cell, J. Biomed. Opt., 3, no.3, 364-372 (1998). DOI:10.1117/1.429883
20. A.A. Savelov, Plane Curves. Systematics, Attributes, Applications. (Handbook) , Gosudarstvennoe Izdatel'stvo Fiziko-Matematicheskoi Literatury, Moscow, 1960. (in Russian)
21. E. Brieskorn, H. Knörrer, Plane Algebraic Curves, Translated by J.Stillwell, Reprint of the 1986 Edition, Birkhäuser, Springer, Basel, 2010. DOI:10.1007/978-3-0348-0493-6
22. P.W. Kuchel, E.D. Fackerell, Parametric-Equation Representation of Biconcave Erythrocytes, Bulletin of Mathematical Biology, 61, 209-220 (1999). DOI:10.1006/bulm.1998.0064
23. I.M. Mladenov, M.Ts. Hadzhilazova, P.A. Djondjorov, V.M. Vassilev, On Some Deformations of the Cassinian Oval, AIP Conf. Proc., 1340, 81-89 (2011). DOI:10.1063/1.3567127
24. A.E. Moskalensky, A.L. Litvinenko, V.M. Nekrasov, M.A. Yurkin, A Physical Model of Blood Platelets Shape and its Effect on Light Scattering, URSI International Symposium on Electromagnetic Theory (EMTS), 585-587 (2016). DOI:10.1109/URSI-EMTS.2016.7571460